

Charge Carrier Transport in Poly(2,5-dialkoxy-*p*-phenylene ethynylene)s

Akshay Kokil,¹ Irina Shiyanovskaya,² Kenneth D. Singer,^{1,2} Christoph Weder¹

¹*Department of Macromolecular Science and Engineering, Case Western Reserve University, Cleveland, OH 44106-7202, USA.*

²*Department of Physics, Case Western Reserve University, Cleveland, OH 44106-7079, USA.*

The charge carrier transport in poly[2,5-dioctyloxy-1,4-diethynyl-phenylene-*alt*-2,5-bis(2'-ethylhexyloxy)-1,4-phenylene], a poly(*p*-phenylene ethynylene) (PPE) derivative, was investigated by time-of-flight measurements. The charge transport characteristics in this material are ambipolar, and the transport is dispersive, with high electron ($2.2 \times 10^{-3} \text{ cm}^2 \text{ V}^{-1} \text{ s}^{-1}$) and hole ($1.8 \times 10^{-3} \text{ cm}^2 \text{ V}^{-1} \text{ s}^{-1}$) mobilities at room temperature and at low field ($3.1 \times 10^4 \text{ V cm}^{-1}$). The mobility strongly depends on the field strength, and is observed to decrease with increasing bias. The positional and energetic disorder parameters were calculated from the temperature and field dependencies of the charge mobility using a Gaussian disorder transport formalism. The positional disorder was found to be larger than the energetic disorder over the entire experimental temperature range, leading to the observed negative field dependence of the carrier mobility.

In the past three decades, π -conjugated semiconducting polymers have attracted significant interest, since these materials may combine the processability and outstanding mechanical properties of polymers with the exceptional, readily tailored electronic and optical properties of functional organic molecules.¹ The potential use of these materials in light-emitting diodes (LED),² field-effect transistors (FET),³ photorefractive devices,⁴ and photovoltaic cells,⁵ have motivated the development of synthesis and processing methods of conjugated polymer materials with unique, field-responsive properties.⁶ Among a variety of materials platforms, poly(*p*-phenylene ethynylene) (PPE) derivatives (Fig. 1) have attracted the attention of a number of research groups.⁷ While the nonlinear optical properties of PPEs have been carefully studied,⁸ and the photoluminescence of these materials has been exploited in sensors⁹ and other devices,¹⁰ the investigation and exploitation of the semiconducting properties of PPEs have, somewhat surprisingly, received relatively little attention.^{11,12,13} Only recently, PPEs have been demonstrated¹⁴ to be more useful in polymer LEDs, than the original experiments had indicated.¹⁵ In connection with the investigation of organometallic polymer networks based on a PPE derivative and Pt⁽⁰⁾,¹⁶ the carrier mobilities in poly[2,5-dioctyloxy-1,4-diethynyl-phenylene-*alt*-2,5,-bis(2'-ethylhexyloxy)-1,4-phenylene] (EHO-OPPE, Fig. 1),¹⁷ a soluble poly(*p*-phenylene ethynylene) derivative have recently attracted our own interest. In this letter, we present a detailed study of the charge transport properties of this material, which is representative of this family of conjugated polymers.

The charge transport in EHO-OPPE was investigated using time-of-flight (TOF) measurements on indium-tin-oxide (ITO)/polymer/gold sandwich structures.¹⁸ In this technique, a short light pulse incident on the polymer through a semitransparent electrode creates a thin sheet of

charge carriers and, depending on the polarity of the electric field E applied between the electrodes, electrons or holes are driven across the sample. The absorption depth of the optical excitation is small compared to the sample thickness L (for the present polymer ca. 1 μm at the wavelength of interest, cf. Ref. 17) and the duration of the optical pulse is short compared to the transit time t_{tr} of the charge carriers. Thus, using $\mu = L / t_{tr} E$ the carrier mobility μ can be obtained from the displacement photocurrent transients. The polymer sample used in the present study was of a number-average molecular weight, M_n , of about 10,000 $\text{g} \cdot \text{mol}^{-1}$, and was synthesized according to standard procedures.¹⁷ ITO / EHO-OPPE / gold sandwich structures were produced by casting a toluene solution of the polymer (10 $\text{mg} \cdot \text{mL}^{-1}$) onto ITO-coated glass-slides (E.H.C. Co., Japan), drying the resulting films *in vacuo* at 40 ° for at least 12 h ($L = 6.5 - 12 \text{ }\mu\text{m}$) and depositing a 3 x 3 mm^2 gold electrode of a thickness of 60 nm by sputtering through a shadow-mask. Dark currents were measured to be in the range of 30-60 nA indicating that carrier injection was negligible. We have shown earlier that the rapid evaporation of the solvent leads to amorphous films, in which the macromolecules are highly disordered [8,17]. The TOF measurements were conducted on a conventional setup,¹⁸ using a 3.6-ns Q-switched Nd-YAG (yttrium aluminum garnet) laser, which was frequency doubled and shifted using a high pressure H_2 Raman cell. The third anti-Stokes shift (320 nm) of the 532 nm pump with an intensity of < 10 $\mu\text{J}/\text{pulse}$ was used for the carrier generation. Typical photocurrent transients are shown in Fig. 2 for electrons and Fig. 3 for holes. The shape of these curves is representative for all transients observed here and is characteristic of dispersive transport.^{19,20,21,22,23} The carrier mobility μ was determined from the inflection point in the double logarithmic plots (Figs. 2B and 3B).¹⁹ TOF measurements were performed as a function of carrier type, applied field and film thickness (Fig.

4). As can be seen from Fig. 4, the drift mobility is independent of L , demonstrating that the photocurrents are not range-limited but indeed reflect the drift of the carrier sheet across the entire sample. (Both the) independence of the mobility on L , and the fact that the slopes of the tangents used to determine the mobility (Figures 2 and 3) do not add to -2 as predicted by the Scher-Montroll theory, indicate that the Scher-Montroll picture of dispersive transients does not adequately describe the data presented here.²⁴ The dispersive nature of the transient is due to the high degree of disorder in the sample and its impact on carrier transport.¹⁹ Although energetic disorder described by a Gaussian density of states certainly contributes to the dispersive shape of the transients²⁵, the independence of μ with L indicates that other types of disorder will also contribute.²⁶ The observed disorder likely arises from the large degree of positional disorder as described below, and perhaps polaron or intrachain mechanisms in these highly conjugated polymers.

High electron ($2.2 \times 10^{-3} \text{ cm}^2 \text{V}^{-1} \text{s}^{-1}$) and hole ($1.8 \times 10^{-3} \text{ cm}^2 \text{V}^{-1} \text{s}^{-1}$) mobilities were found at low field ($3.1 \times 10^4 \text{ Vcm}^{-1}$). This finding is most intriguing, since these values compare favorably with, to our knowledge, the highest values yet observed for an ambipolar conjugated polymer.²⁷ The data plots and fits in Fig. 5 indicate that the temperature dependence is well-described by the Gaussian disorder model presented below. As is evident from Figs. 4A and 4B, the mobility strongly depends on the field strength, and decreases with increasing bias. This somewhat exceptional behavior has been observed before,^{28,29} particularly at low fields, and is consistent with a hopping transport model that accounts for off-diagonal (positional) disorder caused by variations of intersite distances in addition to diagonal (energetic) disorder in the transport manifold.^{30, 31} The disorder transport model considers charge transport in organic solids as time-

independent random walks within a distribution of localized hopping states broadened by disorder effects. The large off-diagonal disorder may result in a negative field dependence of the mobility at low fields, because a stronger applied electric field favors forward hopping and inhibits more facile routes for carriers involving hops transverse to the applied electric field. The negative field dependence was also predicted for quasi one-dimensional transport in the presence of defects and barriers.³²

To analyze the negative field dependence of the mobility in EHO-OPPE within the Gaussian disorder transport formalism and to determine the diagonal (energetic) disorder parameter $\hat{\mathbf{s}}$ and the off-diagonal (positional) disorder parameter Σ , we employed the relationship between the charge mobility \mathbf{m} and the disorder parameters³⁰

$$\mathbf{m}(\hat{\mathbf{s}}, \Sigma, E) = \mathbf{m}_0 \exp \left[- \left(\frac{2}{3} \hat{\mathbf{s}} \right)^2 \right] \exp C (\hat{\mathbf{s}}^2 - \Sigma^2) E^{1/2} \quad (1)$$

where \mathbf{m}_0 is the prefactor mobility, E is the electric field, and C is an empirical constant. The diagonal disorder parameter $\hat{\mathbf{s}}$ is related to the width of the Gaussian density of states \mathbf{s} , as $\hat{\mathbf{s}} = \mathbf{s} / kT$, where k is the Boltzman constant and T is the temperature.

Equation (1) can be represented in the form

$$\ln \mathbf{m} = \mathbf{a}(E) \frac{1}{T^2} + g(E) \quad (2)$$

where

$$\mathbf{a}(E) = \frac{\mathbf{s}^2}{k^2} \left(C\sqrt{E} - \frac{4}{9} \right) \quad (3)$$

and

$$g(E) = \ln \mathbf{m}_0 - C\sqrt{E}\Sigma^2 \quad (4)$$

The experimental temperature dependence of the mobility parametric in the applied electric field (Fig. 5) allows for calculating \mathbf{a} and g for different values of the electric field. Because $\mathbf{a}(E)$ scales linearly with \sqrt{E} , the value $\mathbf{a}_{E=0}$ can be determined by plotting \mathbf{a} vs. \sqrt{E} and then determining the intersection of the linear fit of the data with $E = 0$. Knowing $\mathbf{a}_{E=0}$ allows us to determine the width of density of states \mathbf{s} from the relation

$$\mathbf{s} = \frac{3}{2} k^2 \sqrt{\mathbf{a}_{E=0}} \quad (5)$$

Finally, the implicit function $g(\mathbf{a})$ should be linear, because the derivative $\frac{\partial g}{\partial \mathbf{a}}$ is a constant

$$\frac{\partial g}{\partial \mathbf{a}} = \frac{\frac{\partial g}{\partial \sqrt{E}}}{\frac{\partial \mathbf{a}}{\partial \sqrt{E}}} = \frac{-C\Sigma^2}{C \frac{\mathbf{s}^2}{k^2}} = -\frac{\Sigma^2 k^2}{\mathbf{s}^2} = \mathbf{j} \quad (6)$$

Therefore, calculating the slope $\mathbf{j} = \frac{\partial g}{\partial \mathbf{a}}$ of the plot $g(\mathbf{a})$ allows for the determination of the value of the off-diagonal disorder parameter Σ

$$\Sigma^2 = -\mathbf{j} \frac{\mathbf{s}^2}{k^2} \quad (7)$$

Table 1 shows the calculated values for the density of states at zero field $\mathbf{s}_{E=0}$, the disorder parameters $\hat{\mathbf{s}}$ and Σ , and the constant C for holes and electrons in EHO-OPPE. Fig. 6 displays the temperature dependence of the diagonal disorder parameter $\hat{\mathbf{s}}$. It is apparent from the data presented in Table 1 and in Fig. 6 that the off-diagonal disorder parameter Σ is larger than diagonal disorder parameter over the entire experimental temperature range. The temperature-independent off-diagonal disorder parameter Σ was 3.4 and 3.6 for electrons and

holes, respectively, while the range of the temperature-dependent diagonal disorder parameter $\hat{\Sigma}$ was between 2.8 and 2.5 and 3.0 and 2.7 in the temperature range between 20 and 50 °C for electrons and holes, respectively. Monte Carlo simulations of carrier hopping in the transport manifold with energy levels with a Gaussian distribution^{28,31} predicted that for large Σ , $\partial \ln \mathbf{a} / \partial \sqrt{E}$ becomes negative at low electric fields ($E \leq 5 \times 10^5 \text{ V/cm}$) and does not obey conventional Poole-Frenkel law $\ln \mathbf{m} \sim \sqrt{E}$. At higher fields $\partial \ln \mathbf{a} / \partial \sqrt{E}$ becomes positive and gives rise to Poole-Frenkel-like behavior. While we were not able to measure the mobility at higher fields because of the dielectric breakdown of the material, the observed negative field dependence of the mobility in conjugated polymer EHO-OPPE with high off-diagonal disorder is consistent with the disorder transport formalism applied to a system with both positional and energetic disorders.

In summary, we have shown that the π -conjugated semiconducting polymer EHO-OPPE exhibits high ambipolar mobility. The positional (off-diagonal) and energetic (diagonal) disorder parameters have been calculated from the experimental temperature and field dependences of the hole and electron mobilities. The observed negative field dependence of the mobility was explained within the Gaussian disorder formalism to originate from high off-diagonal disorder. The experimental temperature and field dependent mobilities are consistent with a Gaussian disorder transport formalism applied to systems exhibiting both positional and energetic disorders.

Acknowledgements

This work was supported by a DuPont Science & Engineering Grant (C.W.), funding from the Case School of Engineering (C.W.), the Goodyear Tire and Rubber Company (C.W.), and a grant from the Air Force Office of Scientific Research, Air Force Material Command, USAF (F49620-99-1-0018) and the New Energy and Industrial Technology Development Organization of Japan (K.S.).

References and Notes

- ¹ A. J. Heeger, *J. Phys. Chem.* 105 (2001) 8475.
- ² (a) A. Kraft, A. C. Grimsdale, A. B. Holmes, *Angew. Chem. Int. Ed.* 37 (1998) 403; (b) U. Mitschke P. Bäuerle, *J. Mater. Chem.* 10 (2000) 1471; (c) A. Greiner C. Weder *Application of Polymeric Materials in LEDs*, in *Encyclopedia of Polymer Science and Technology*, edited by J. I. Kroschwitz (Wiley-Interscience, New York, 2001).
- ³ G. Horowitz, *Adv. Mater.* 10 (1998) 365.
- ⁴ W. E. Moerner, S. M. Silence, *Chem. Rev.* 94 (1994) 127.
- ⁵ C. J. Brabec, N. S. Sariciftci, J. C. Hummelen, *Adv. Funct. Mater.* 11 (2001) 15.
- ⁶ (a) *Handbook of Conducting Polymers*, 2nd Edition, edited by T. J. Skotheim, R. L. Elsenbaumer, J. R. Reynolds (Dekker, New York, 1998); (b) *Handbook of Organic Conductive Molecules and Polymers*, edited by H. S. Nalwa (John Wiley & Sons, New York, 1996); (c) *Physical Properties of Polymers Handbook*, edited by J.A. Mark (American Institute of Physics, New York, 1996).
- ⁷ (a) R. Giesa, *J.M.S.-Rev. Macromol. Chem. Phys.* C36 (1996) 631. (b) U. H. F. Bunz, *Chem. Rev.* 100 (2000) 1605.
- ⁸ (a) C. Weder, M. S. Wrighton, R. Spreiter, C. Bosshard, P. Günter, *J. Phys. Chem.* 100 (1996) 18931; (b) G. S. He, C. Weder, P. Smith, P. N. Prasad, *IEEE J. Quantum Electron.* 34 (1998) 2279.

- ⁹ (a) Q. Zhou, T.M. Swager, *J. Am. Chem. Soc.* 117 (1995) 7017; (b) Q. Zhou, T. M. Swager, *J. Am. Chem. Soc.* 117 (1995) 12593; (c) D. T. Mc. Quade, A. E. Pullen, T.M. Swager, *Chem. Rev.* 100 (2000) 2537.
- ¹⁰ C. Weder, C. Sarwa, A. Montali, C. Bastiaansen, P. Smith, *Science* 279 (1998) 835.
- ¹¹ Q. - X. Ni *et al.* *Synth. Met.* 49-50 (1992) 448.
- ¹² D. Ofer, T. M. Swager, M. S. Wrighton, *Chem. Mater.* 7 (1995) 418.
- ¹³ U. Evans *et al.* *Analyst* 126 (2001) 508.
- ¹⁴ (a) A. Montali, P. Smith, C. Weder, *Synth. Met.* 97 (1998) 123; (b) C. Schmitz *et al.* *Adv. Funct. Mater.* 11 (2001) 41; (c) N. G. Pschirer *et al.* *Chem. Mater.* 13 (2001) 2691.
- ¹⁵ (a) L. S. Swanson, F. Lu, J. Shinar, Y. W. Ding, T. J. Barton, *Proc. SPIE.* 1910 (1993) 101; (b) L. S. Swanson J. Shinar, *Proc. SPIE.* 1910 (1993) 147. (c) L. S. Swanson, J. Shinar, Y. W. Ding, T. J. Barton, *Synth. Met.* 55-57 (1993) 1.
- ¹⁶ A. Kokil, I. Shiyankovskaya, K. D. Singer, C. Weder, *J. Am. Chem. Soc.* In press.
- ¹⁷ C. Weder, M.S. Wrighton, *Macromolecules* 29 (1996) 5157.
- ¹⁸ I. Shiyankovskaya, K. D. Singer, R. J. Twieg, L. Sukhomlinova, V. Gettwert, *Phys Rev E* 65 (2002) 41715.
- ¹⁹ P.M. Borsenberger and D.S. Weiss, *Organic Photoreceptors for Xerography* (Marcel Dekker, New York, 1998).
- ²⁰ E. Lebedev, T. Dittrich, V. Petrova-Koch, S. Karg, W. Brütting, *Appl. Phys. Lett.* 71 (1997) 2686.
- ²¹ D. Hertel, H. Bässler, U. Scherf, H.H. Hörhold, *J. Chem. Phys.* 110 (1999) 9214.

- ²² I. H. Campbell, D. L. Smith, C. J. Neef, J. P. Ferraris, *Appl. Phys. Lett.* 74 (1999) 2809.
- ²³ A. R. Inigo *et al.*, *Adv. Mater.* 13 (2001) 504.
- ²⁴ H. Scher, E.W. Montroll, *Phys. Rev. B* 12 (1975) 2455.
- ²⁵ P. M. Borsenberger, L. Pautmeier, H. Bässler, *Phys. Rev. B* 46, (1992) 12145.
- ²⁶ J.C. Scott, L. Pautmeier, and L.B. Schein, *Phys. Rev. B* 46, (1992) 8603.
- ²⁷ A. M. Babel, S. A. Jenekhe, *Adv. Mater.* 14 (2002) 371.
- ²⁸ P. M. Borsenberger, L. Pautmeier, H. Bässler, *J. Chem. Phys.* 94 (1991) 5447.
- ²⁹ D. Hertel, H. Bässler, U. Scherf, H. H. Hörhold, *J. Chem. Phys.* 110 (1999) 9214.
- ³⁰ H. Bässler, *Phys. Stat. Sol (b)* 175 (1993) 15.
- ³¹ L. Pautmeier, R. Richert, H. Bässler, *Synth. Met.* 37 (1990) 271.
- ³² B. Movaghar, D. W. Murray, K. J. Donovan, E. G. Wilson, *J. Phys. C: Solid State Phys.* 17 (1984) 1247.

Table 1. Results of data fits to the Gaussian disorder model of charge transport.

Charge carrier	$s_{E=0}$ (eV)	Σ	$\hat{s}_{20^\circ C}$	$C(\text{cm/V})^{1/2}$
Holes	0.072	3.6	3.0	5.4×10^{-4}
Electrons	0.068	3.4	2.8	5.7×10^{-4}

Figure Captions

- Fig. 1.** Molecular structure of poly[2,5-dioctyloxy-1,4-diethynyl-phenylene-*alt*-2,5-bis(2'-ethylhexyloxy)-1,4-phenylene] (EHO-OPPE), the poly(*p*-phenylene ethynylene) (PPE) derivative investigated here.
- Fig. 2.** Electron time-of-flight photocurrent transients of solution-cast film of EHO-OPPE ($L=8\ \mu\text{m}$), measured at 295 K and an electric field of $2.5\times 10^5\ \text{Vcm}^{-1}$ in a (A) linear and (B) double logarithmic plot.
- Fig. 3.** Hole time-of-flight photocurrent transients of solution-cast films of EHO-OPPE ($L=8\ \mu\text{m}$), measured at 295 K and the electric field of $2.5\times 10^5\ \text{Vcm}^{-1}$ in a (A) linear and (B) double logarithmic plot.
- Fig. 4.** Electron (A) and hole (B) mobilities of EHO-OPPE-films as function of electric field at various film thicknesses (open triangles: $L=6.5\ \mu\text{m}$, filled circles: $L=8\ \mu\text{m}$, open squares: $L=12\ \mu\text{m}$).
- Fig. 5.** Temperature dependence of (A) electron and (B) hole mobilities of an EHO-OPPE film ($L=8\ \mu\text{m}$) measured at $E = 2\times 10^5$ (squares), 3×10^5 (circles) and $4\times 10^5\ \text{Vcm}^{-1}$ (triangles).

Fig. 6. Temperature dependence of the diagonal disorder parameter \hat{S} for holes (squares) and electrons (circles). Parameters have been obtained by fitting the experimental data (Fig. 5) to Eqs. 1 and 5.

Figure 1

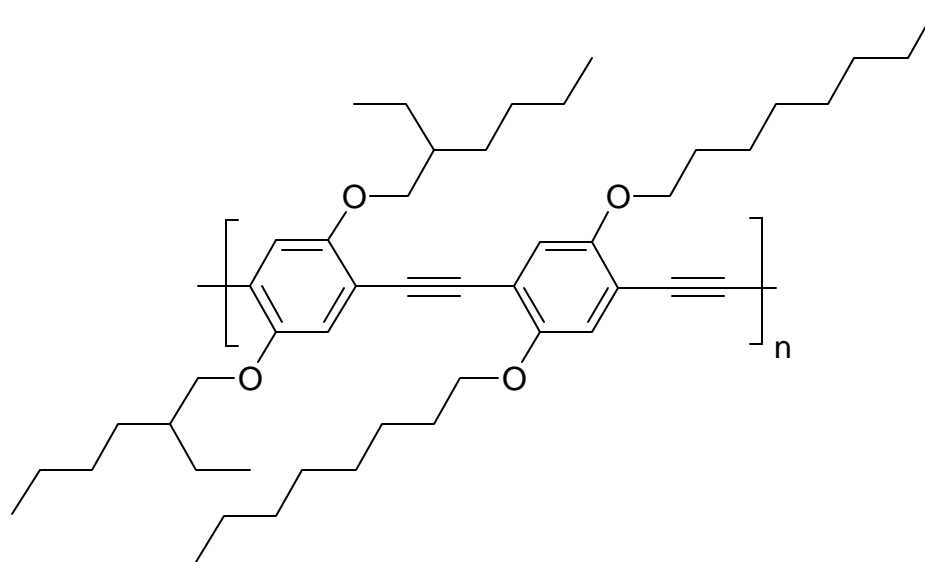


Figure 2

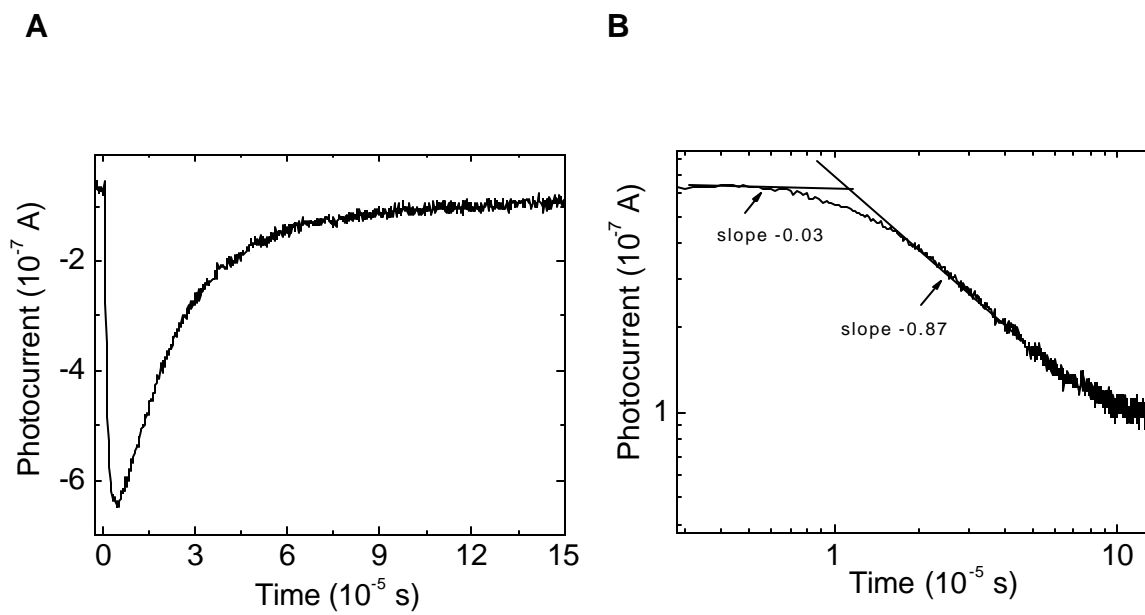


Figure 3

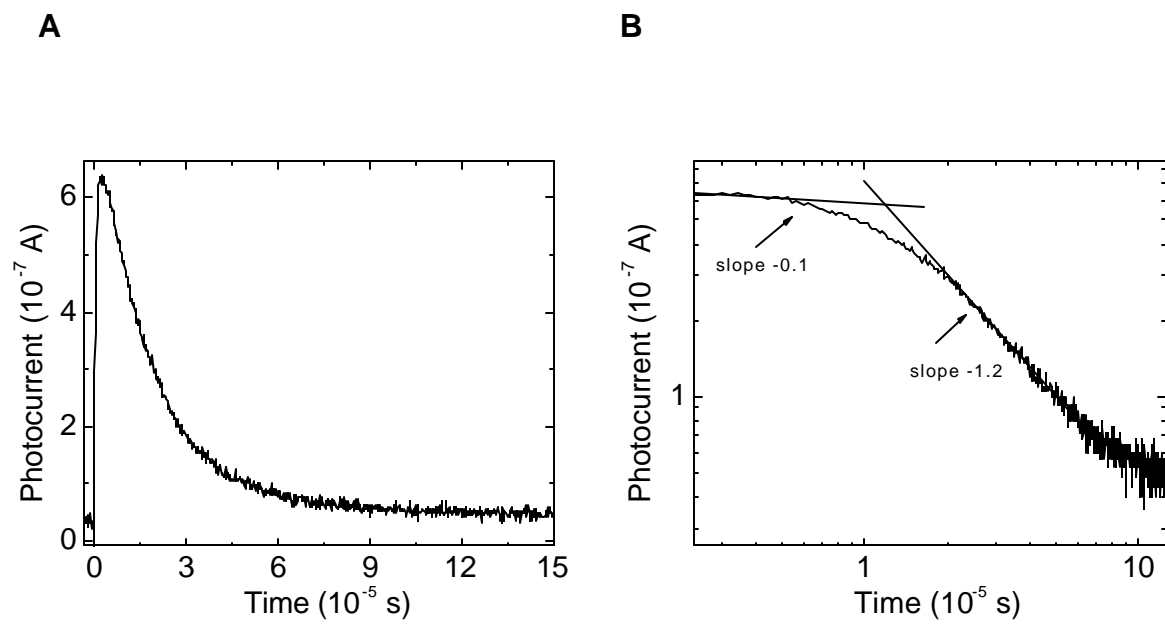


Figure 4

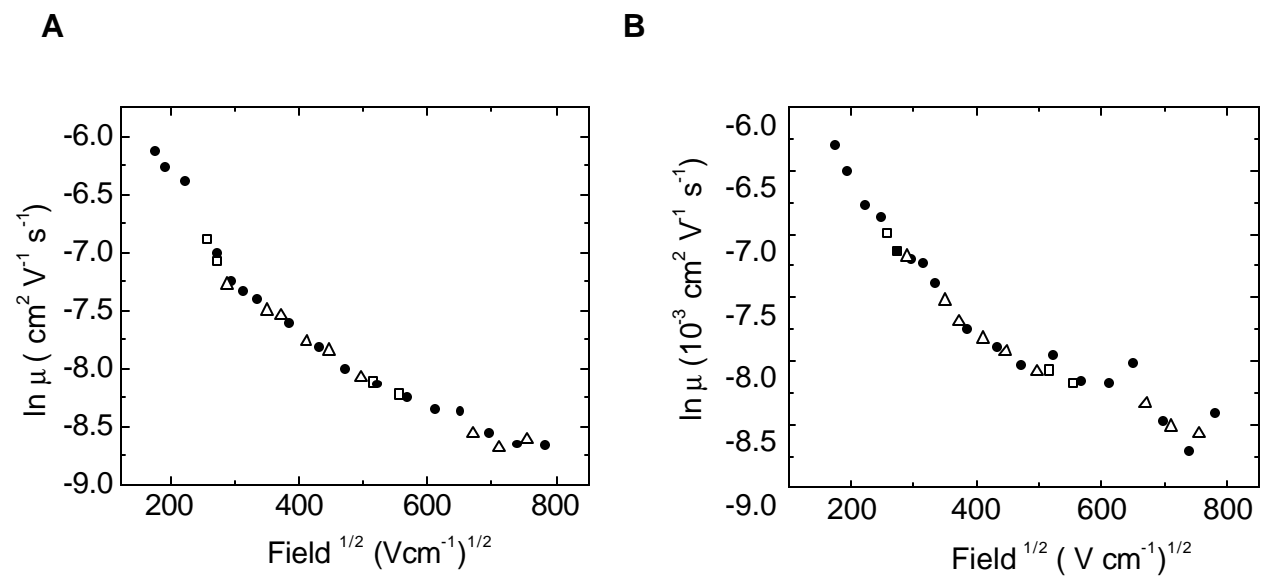
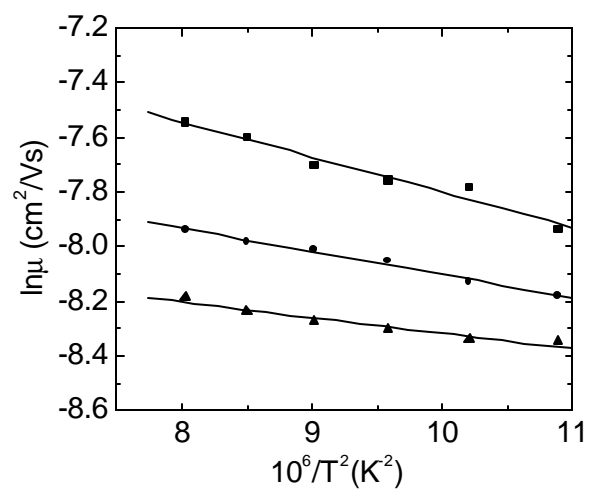


Figure 5

A



B

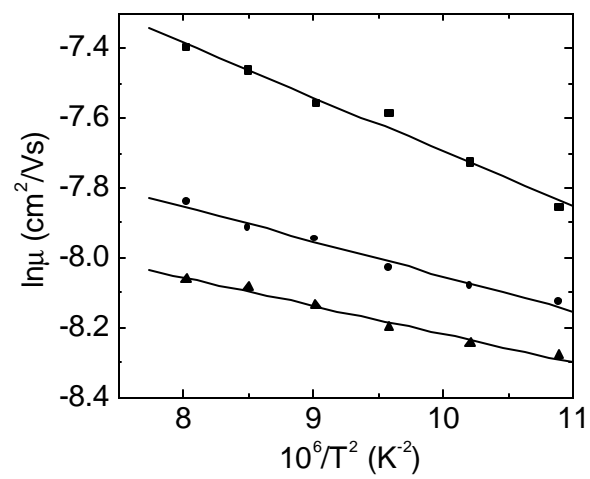


Figure 6

